

Self-Assembling Bipyridinium Multilayers

Robert J. Alvarado, Jhindan Mukherjee, Eden J. Pacsial, Daniel Alexander, and Francisco M. Raymo*

Center for Supramolecular Science, Department of Chemistry, University of Miami, 1301 Memorial Drive, Florida 33146-0431

Received: November 13, 2004; In Final Form: February 3, 2005

The identification of strategies to assemble nanostructured films with engineered properties on solid supports can lead to the development of innovative functional materials. In particular, the self-assembly of electroactive multilayers from simple molecular building blocks on metallic electrodes can offer the opportunity to regulate the exchange of electrons between the underlying substrate and solution species. In this context, we designed an experimental protocol to prepare electroactive films from bipyridinium bisthiols. Specifically, we found that a compound incorporating two bipyridinium dications at its core and terminal thiol groups self-assembles into remarkably stable multilayers on polycrystalline gold. The surface coverage of the resulting films can be regulated by adjusting the exposure time of the gold substrate to the bipyridinium solution. Control experiments with appropriate model compounds demonstrate that both bipyridinium dications as well as both thiol groups must be present in the molecular skeleton to encourage multilayer growth. The resulting films transport electrons efficiently from the electrode surface to the film/solution interface. Indeed, they mediate the reduction of $\text{Ru}(\text{NH}_3)_6^{3+}$ in the electrolyte solution but prevent the back oxidation of the resulting $\text{Ru}(\text{NH}_3)_6^{2+}$. Furthermore, these polycationic bipyridinium films capture electrostatically $\text{Fe}(\text{CN})_6^{4-}$ tetraanions, which can also be exploited to transport electrons across the interfacial assembly. In fact, electrons can travel through the bipyridinium $^{2+/1+}$ couples to redox probes in solution and then back to the electrode through the $\text{Fe}(\text{CN})_6^{4/3-}$ couples. Thus, our original approach to self-assembling multilayers can produce stable electroactive films with unique electron transport properties, which can be regulated with a careful choice of the anionic components.

Introduction

The need to understand the fundamental factors regulating interfacial electron transfer¹ has stimulated the development of experimental protocols to coat the surface of metallic and semiconducting electrodes with molecular films.² The resulting coatings alter significantly the ability of the underlying electrodes to exchange electrons and holes with redox probes in solution. Thus, the rationalization of their basic properties can evolve into the identification of viable principles to control electron transport at interfaces. In turn, strategies to regulate interfacial electron transfer can have profound technological implications in corrosion prevention, electroanalysis, electrocatalysis, energy conversion, and nanoelectronics. These fascinating prospects have encouraged intense research efforts directed specifically to the modification of electrodes with electroactive films and the analysis of their electrochemical response.

Redox polymers are convenient building blocks for the preparation of electroactive films.^{2,3} Indeed, relatively simple casting or spin-coating procedures facilitate the deposition of preformed polymers, incorporating multiple redox sites along their backbones, on a diversity of substrates. Alternatively, analogous protocols can be employed to coat electrodes with charged polymers. The subsequent exchange of their counterions with electroactive ions results in the electrostatic confinement of redox sites on the electrode surface. Similar films are also

produced from molecular precursors after electropolymerizations or polycondensations at electrode/solution interfaces. In all instances, the final interfacial assemblies span from a few nanometers to several micrometers in thickness and incorporate multiple layers of randomly oriented redox sites.

Arrays of ordered redox sites can be prepared relying on the Langmuir–Blodgett technique.^{2a,4} The sequential transfer of electroactive monolayers from air/water interfaces to solid supports results in the gradual construction of organized multilayers. Similarly, the layer-by-layer assembly of electroactive films can be achieved by exposing reiteratively electrodes to polycationic and polyanionic components.⁵ Electrostatic forces between the complementary polymers assist the sequential growth of these interfacial assemblies. The repetitive nature of both strategies, however, translates into labor-intensive experimental protocols.

The self-assembly of disulfides, thioethers, and thiols on gold does not require external intervention, other than the simple exposure of the solid substrate to the adsorbing building block.⁶ These spontaneous processes, therefore, are particularly attractive for the attachment of redox-active molecules to electrodes.⁷ The resulting interfacial assemblies are ideal model systems for the elucidation of the stereoelectronic factors ruling heterogeneous electron transfer. However, a single molecular layer can only be formed on the electrode surface in most instances. The low surface coverages associated with these electroactive monolayers translate in modest signal-to-noise ratios and limited stability in comparison to the otherwise robust and thick multilayer films.

* Author to whom correspondence should be addressed. Phone: (305) 284-2639. Fax: (305) 284-4571. E-Mail: fraymo@miami.edu.

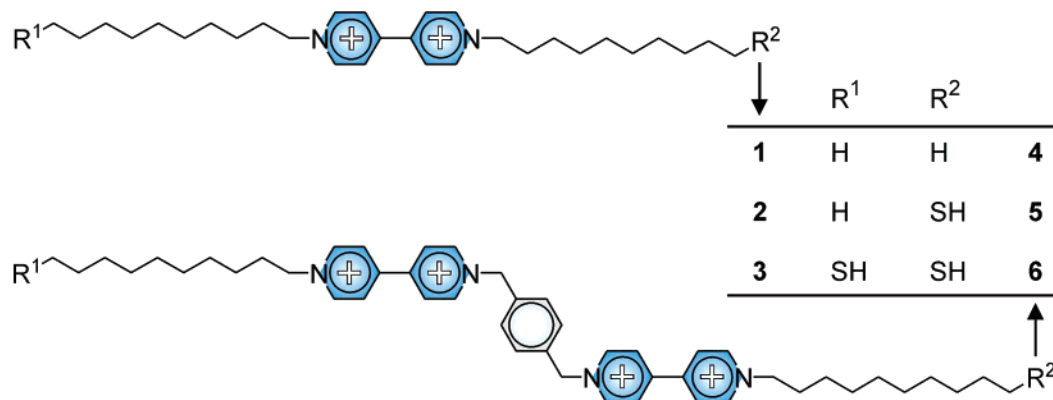


Figure 1. Electroactive building blocks incorporating one (1–3) or two (4–6) bipyridinium dications.

Recent studies recognized the ability of certain 1,*n*-alkanedithiols⁸ and 1,*n*-areneedithiols⁹ to form multilayers on gold. These processes involve the initial formation of monolayers, after gold–thiolate bonding at one end of the bisthiols. The remaining thiol groups protrude away from the underlying substrates and encourage the adsorption of multiple overlayers, after oxidative disulfide bonding. Thus, the simple immersion of a gold substrate in a solution of a bisthiol can result in the spontaneous growth of multilayer assemblies at the solid/liquid interface. On the basis of these observations, we realized that a redox-active bisthiol should be able to adsorb on gold electrodes and, under appropriate experimental conditions, produce relatively thick films after the spontaneous formation of disulfide linkages. In principle, this strategy should provide access to electroactive multilayers in a single experimental step, relying on the efficiency and simplicity of self-assembly. In this article, we report the experimental implementation of our innovative approach to electroactive films and illustrate the electron transport properties of the resulting interfacial assemblies.

Experimental Procedures

Methods and Materials. The bipyridinium compounds 1–6 were synthesized according to the procedures in the Supporting Information (Figures S1–S6). The other chemicals and materials employed were purchased from commercial sources and used as received. Water (18.2 MΩ cm) was purified with a Barnstead International Nanopure Diamond Analytical system. The electrochemical measurements were performed in aqueous electrolytes using a CH Instruments 660 workstation. The impedance profiles were recorded after maintaining the voltage of the electrode at the half-wave potential of the redox couple for 600 s.

Gold Electrodes. Polycrystalline gold disk electrodes (CH Instruments 101P) were polished with an Al₂O₃ slurry (0.05 μm), rinsed with H₂O, sonicated for 2 min in H₂O, rinsed with H₂O and MeOH, and dried in a stream of Ar. Then, they were integrated in a two-electrode cell filled with aqueous KOH (3 M). The potential was cycled 10 times between 0 and −2 V relative to a platinum counter electrode. At this point, the gold electrodes were rinsed with H₂O, polished with an Al₂O₃ slurry (0.05 μm), rinsed with H₂O, sonicated for 2 min in H₂O, rinsed with H₂O, maintained in concentrated H₂SO₄ at 40 °C for 10 min, rinsed with H₂O and MeOH, and dried in a stream of Ar.

Film Preparation. The pretreated gold electrodes were immersed in chloroform/methanol (2:1) solutions (0.3 mM) of one of the bipyridinium compounds 1–6 for 1–72 h. Then, they were rinsed with MeOH, CHCl₃, MeOH, H₂O, and MeOH and dried under a stream of Ar. The modified electrodes were

integrated in a conventional three-electrode cell filled with aqueous KCl (0.1 M) and fitted with a platinum counter electrode and a Ag/AgCl reference electrode.

Results and Discussion

Design and Synthesis. Bipyridinium dications undergo two consecutive mono-electronic reductions at moderate potentials.¹⁰ Their reliable electrochemical response survives the incorporation in redox polymers, Langmuir–Blodgett films, layer-by-layer assemblies, and monolayers.¹¹ These reasons encouraged us to design potential building blocks for self-assembling multilayers around the unique properties of bipyridinium dications. Specifically, we identified six compounds (Figure 1) differing in the number of bipyridinium dications per molecule and in the functional groups at the termini of their oligomethylene chains. The dications 1–3 incorporate only one bipyridinium unit at their core, while the tetracations 4–6 have two electroactive sites linked by a central *p*-phenylene bridge. Both oligomethylene chains of 1 and 4 are terminated by methyl groups, while those of 3 and 6 both have a thiol group at their end. Compounds 2 and 5, instead, have a methyl at one end and a thiol group at the other. The sulfur-containing functional groups are expected to anchor the bipyridinium sites to the surface of gold electrodes. Furthermore, they are supposed to promote multilayer growth through disulfide formation in the case of 3 and 6.

We isolated the chloride salts of the bipyridinium cations 1–6 after multistep synthetic procedures (Figures S1–S6, Supporting Information), involving the initial N-alkylation of 4,4′-bipyridine at one or both nitrogen atoms. In the case of the symmetric dications 1 and 3, the heterocyclic core was bisalkylated in a single step by reacting 4,4′-bipyridine with an excess of either 10-bromodecane or 10-iododecyl thioacetate. The asymmetric bipyridinium dications of 2, 4, and 6 were assembled in two consecutive N-alkylation steps. Instead, the synthesis of the asymmetric compound 5 demanded a sequence of four N-alkylation steps. The thiol groups of 2, 3, 5, and 6 were generated in the final step of their syntheses, after transesterification of the corresponding thioacetates under mild acidic conditions.

Monolayer and Multilayer Formation. We compared the abilities of the bipyridinium building blocks 1–6 to adsorb on gold under identical experimental conditions. Specifically, we maintained polycrystalline gold electrodes in chloroform/methanol (2:1) solutions of the six bipyridinium compounds (0.3 mM) for immersion times ranging from 1 to 72 h. Then, we rinsed the gold substrates with various solvents, integrated them in conventional three-electrode cells, and recorded their cyclic voltammograms.

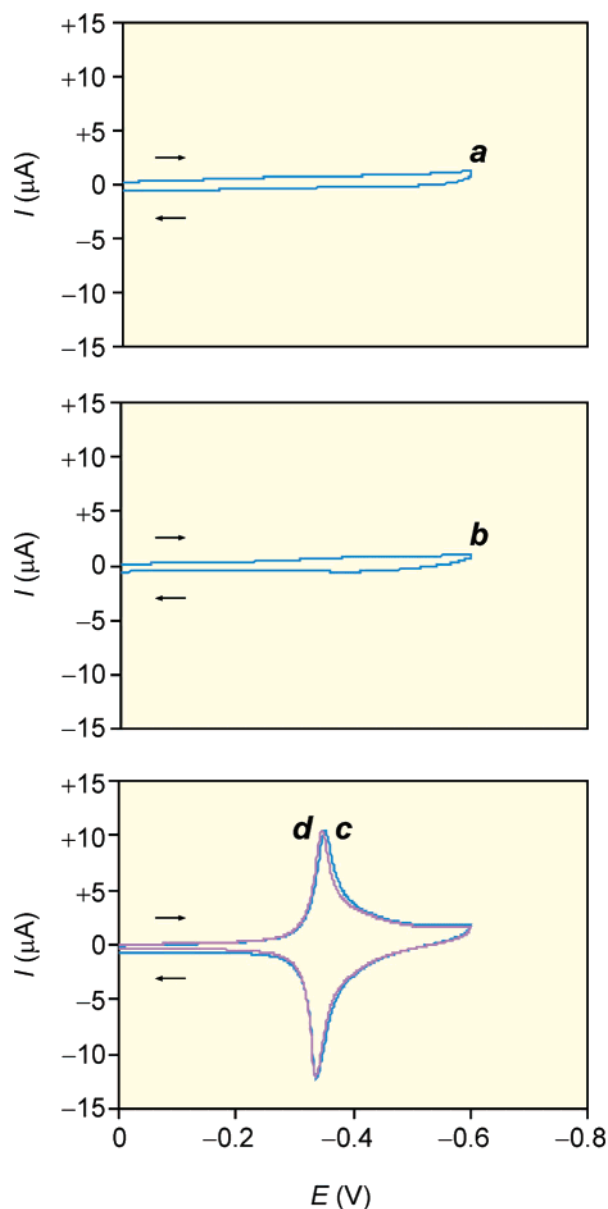


Figure 2. Cyclic voltammograms (0.1 M KCl_{aq}, 100 mV s⁻¹, V vs Ag/AgCl) recorded after the immersion of gold working electrodes in solutions of (a) **1** for 72 h, (b) **2** for 48 h, and (c) **3** for 24 or (d) 48 h followed by copious rinsing.

We found that compounds **1** and **4**, lacking thiol groups at the termini of their oligomethylene tails, do not adsorb on the surface of the working electrodes. The corresponding cyclic voltammograms (Figures 2a and 3a) do not show the characteristic waves for the reversible reduction of bipyridinium dications.^{10,11} We observed a similar result for the dication **2** (Figure 2b). Despite its thiol group, this compound does not adsorb on gold under our experimental conditions. Presumably, the relatively high solubility of **2** in chloroform/methanol (2:1) prevents this particular thiol from adsorbing on the electrode surface.

In contrast to compounds **1**, **2**, and **4**, the dicationic bisthiol **3** adsorbs on the surface of polycrystalline gold electrodes under otherwise identical conditions. The cyclic voltammogram (Figure 2c) of the resulting film reveals waves for the mono-electronic reduction of the bipyridinium dications and for the back oxidation of the corresponding radical cations. The half-wave potential ($E_{1/2}$) is -0.34 V with a peak splitting (ΔE_p) of 15 mV at 100 mV s⁻¹ (Table 1). The cyclic voltammogram

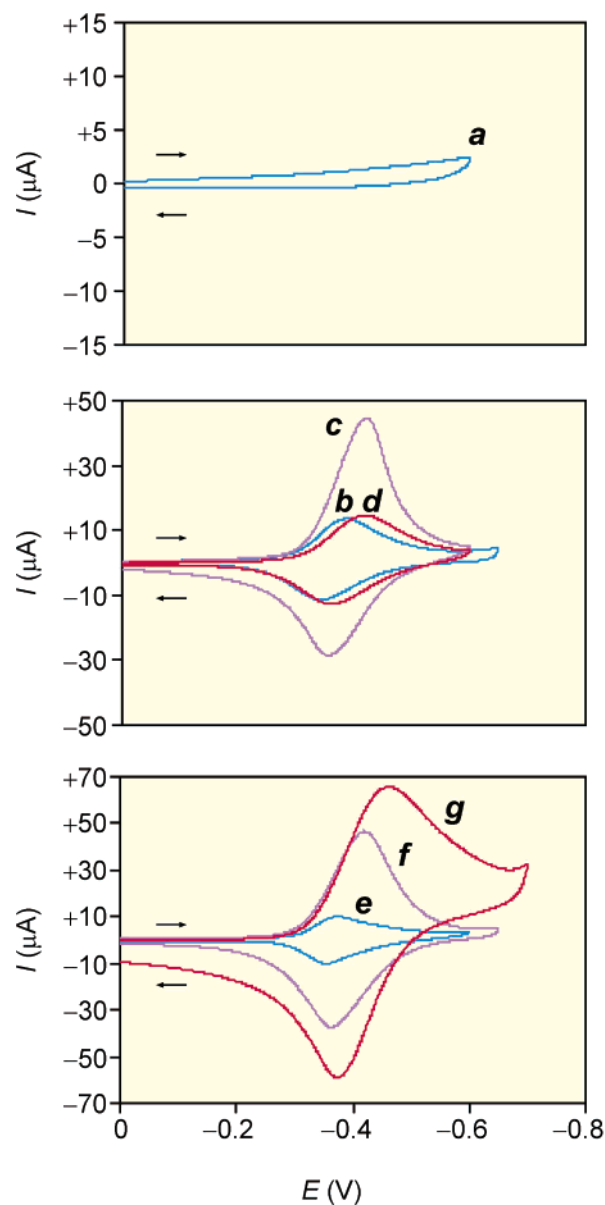


Figure 3. Cyclic voltammograms (0.1 M KCl_{aq}, 100 mV s⁻¹, V vs Ag/AgCl) recorded after the immersion of gold working electrodes in solutions of (a) **4** for 72 h, (b) **5** for 24 or (c and d) 48 h, and (e) **6** for 1, (f) 6, or (g) 48 h. All voltammograms were determined after extensive rinsing of the electrodes with the exception of c.

remains essentially unchanged, if the immersion time of the gold substrate in the bipyridinium solution is prolonged from 24 to 48 h (Figures 2c and 2d). Furthermore, the peak current increases linearly with the scan rate (Figure 4a), and the slope (A) of the corresponding logarithmic plot is 0.89 (Table 1). The surface coverage (Γ), determined from the redox charge in the cyclic voltammogram, is ca. 0.6 nmol cm⁻² (Table 1). This value includes a correction to account for the roughness of the gold substrate¹² and is close to the limiting Γ expected for a bipyridinium monolayer, which is 0.4 nmol cm⁻².¹³ In summary, this particular compound adsorbs spontaneously on gold but can only form a monolayer, at least under the experimental conditions employed, with a typical thin-layer response.^{2a,c,11b}

In analogy to the dicationic bisthiol **3**, also the tetracationic monothiol **5** adsorbs on polycrystalline gold substrates. Once again, the cyclic voltammogram (Figure 3b) shows waves for the reversible reduction of the bipyridinium dications with an $E_{1/2}$ of -0.37 V and a ΔE_p of 44 mV at 100 mV s⁻¹ (Table 1). In this particular instance, however, an increase in immersion

TABLE 1: Electrochemical Data for Bipyridinium Monolayers and Multilayers Adsorbed on Polycrystalline Gold Electrodes

compound	t^a (h)	$E_{1/2}^b$ (V)	ΔE_p^b (mV)	A^c	Γ^d (nmol cm $^{-2}$)
3	24	−0.34	15		0.59
	48	−0.34	11	0.89	0.60
5	24	−0.37	44		0.64
	48	−0.39	58	0.81	0.67
6	1	−0.36	19	0.90	0.66
	6	−0.39	57	0.73	2.52
	48	−0.42	90	0.68	8.43

^a Exposure time (t) of the gold substrate to the bipyridinium solution.

^b Half-wave potential ($E_{1/2}$) and peak splitting (ΔE_p) in the cyclic voltammograms measured at a scan rate of 100 mV s $^{-1}$. ^c Slope (A) of the logarithmic plot of the peak current in the cyclic voltammogram against the scan rate. ^d Surface coverage (Γ) estimated from the cyclic voltammograms measured at a scan rate of 10 mV s $^{-1}$ with the exception of the second and last entries, which were determined at scan rates of 100 and 1 mV s $^{-1}$, respectively. The Γ values include a correction to account for surface roughness, which was 4.0 ± 0.8 for the gold substrates employed.

time from 24 to 48 h results in a dramatic enhancement of the peak current (Figure 3c). Indeed, the transition from the dication **3** to the tetracation **5** translates into a significant solubility decrease of the bipyridinium building block in the deposition solvent. Consequently, a prolonged immersion time tends to encourage the accumulation of the tetracation **5** on the electrode surface. Nonetheless, the peak current drops by 63%, after extensive rinsing of the electrode surface, and the cyclic voltammogram (Figure 3d) becomes similar to the one recorded after 24 h (Figure 3b). The resulting film shows a thin-layer response with a linear correlation between peak current and scan rate (Figure 4b) and an A of 0.81 (Table 1). In agreement with the formation of a single electroactive layer, Γ determined after either 24 or 48 h is again ca. 0.6 nmol cm $^{-2}$ (Table 1). Thus, this particular compound forms spontaneously electroactive films with large surface coverages over prolonged immersion times, which reduce to stable monolayers after rinsing.

In analogy to the dication **3** and the tetracation **5**, the bisthiol **6** adsorbs on the surface of polycrystalline gold.¹⁴ After an immersion time of only 1 h, the cyclic voltammogram (Figure 3e) reveals the characteristic bipyridinium response with an $E_{1/2}$ of −0.36 V and a ΔE_p of 19 mV at 100 mV s $^{-1}$ (Table 1). The peak current increases linearly with the scan rate (Figure 4c) with an A of 0.90. Once again, the value of Γ is close to 0.6 nmol cm $^{-2}$ (Table 1) and is consistent with the formation of a monolayer on the electrode surface. As observed for the tetracation **5**, the cyclic voltammogram shows a pronounced dependence on the immersion time. The peak current increases significantly, if the exposure time is prolonged to 6 and 48 h (Figures 3f and 3g). In this instance, however, rinsing has no influence on the electrochemical response of the bipyridinium dications. In fact, the redox waves in the cyclic voltammogram remain essentially unaltered after (1) multiple reduction/oxidation cycles, (2) extensive washing of the electrode surface with chloroform, methanol, and water, (3) storage of the modified substrates in air for weeks, or (4) prolonged immersion of the films in organic or aqueous solvents. The increase in peak current with immersion time is accompanied by negative shifts in $E_{1/2}$ and enhancements in ΔE_p (Table 1). Furthermore, the bipyridinium response is clearly under diffusion control^{12a,c,11b} with noticeable deviations from linearity of the scan-rate dependence of the peak current (Figures 4d and 4e) and A values of only 0.73 and 0.68 (Table 1). Consistent with the formation of multiple electroactive layers on the electrode surface, the Γ

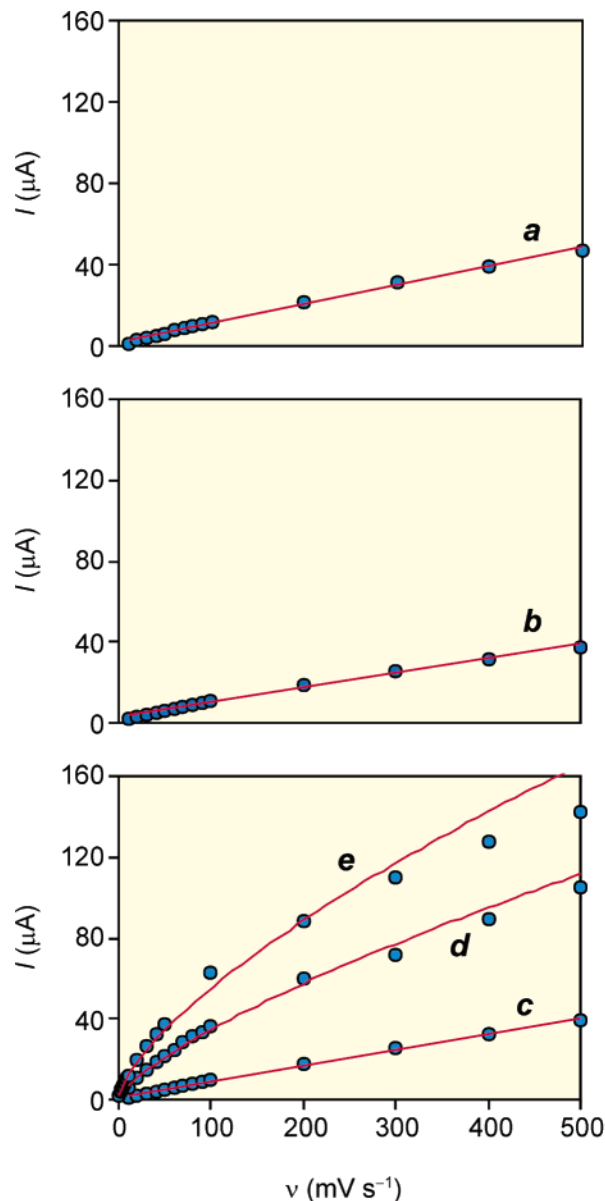


Figure 4. Scan-rate dependence of the peak currents in the cyclic voltammograms (0.1 M KCl_{aq}) recorded after the immersion of gold working electrodes in solutions of (a) **3** for 48 h, (b) **5** for 48 h, or (c) **6** for 1, (d) **6**, or (e) 48 h followed by copious rinsing.

values determined from the voltammetric waves at slow scan rates are ca. 2.5 and 8.4 nmol cm $^{-2}$ (Table 1). These values are approximately 4 and 13 times higher than the average (0.63 nmol cm $^{-2}$) of the surface coverages in Table 1 for monolayers of **3**, **5**, and **6**. Thus, the relatively low solubility of the tetracation **6** encourages its adsorption on gold beyond monolayer surface coverages, after prolonged immersion times, to form remarkably stable electroactive films. Of course, the only structural difference between the tetracations **5** and **6** is the presence of an additional thiol group in **6**. This particular functional group must be responsible for imposing stability on the electroactive multilayers formed by **6**, which otherwise desorb easily in the case of **5**. It is reasonable to assume that interlayer disulfide bonding is responsible for the behavior of the bisthiol **6**. In fact, this mechanism is known to encourage the assembly of 1, n -alkanedithiols⁸ and 1, n -areneedithiols⁹ into multilayers. Consistent with this interpretation, the evolution of the ^1H NMR spectrum of **6** in chloroform- d_4 /methanol- d_4 (2:1) confirms the oxidative formation of disulfides under these

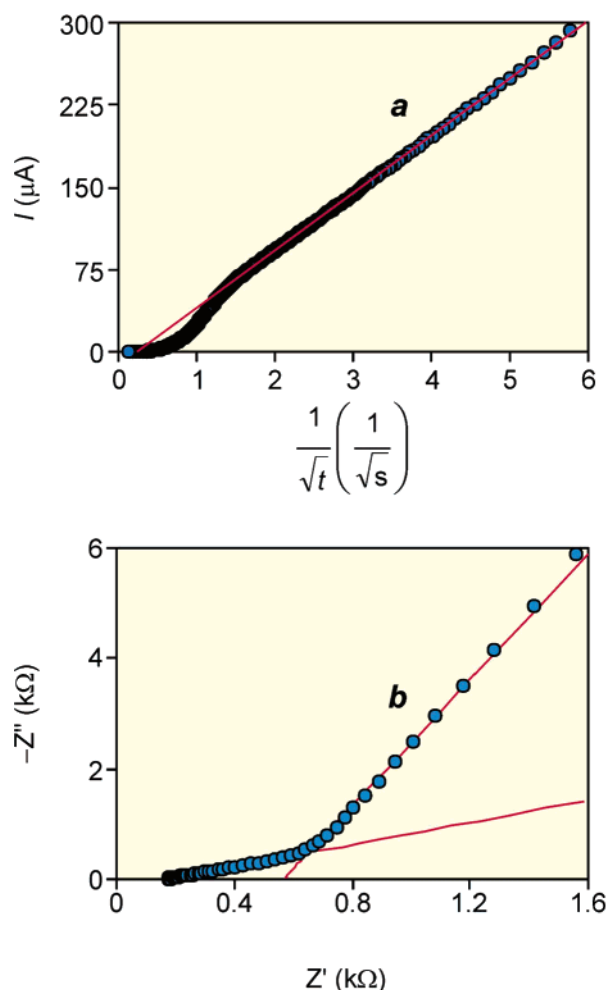


Figure 5. (a) Chronoamperometric ($0 \rightarrow -0.65$ V vs Ag/AgCl) and (b) impedance (-0.418 ± 0.005 V vs Ag/AgCl, 100 kHz–0.1 Hz) plots recorded in KCl_{aq} (0.1 M) after the immersion of gold working electrodes in solutions of **6** for 48 h followed by copious rinsing. The coefficients of determination for the fittings are greater than 0.99.

experimental conditions. In particular, the triplet at 2.46 ppm for the methylene protons adjacent to the terminal thiol groups fades over the course of ca. 5 days with the concomitant development of another triplet at 2.62 ppm. The observed increase in chemical shift for the methylene protons is a characteristic indication of disulfide formation.¹⁵

Electron Transport. The cyclic voltammogram (Figure 3g), recorded after exposing a gold working electrode to a solution of **6** for 48 h, and the scan-rate dependence of the associated peak current (Figure 4e) demonstrate that the response of the resulting film is under diffusion control.^{2a,c,11b} These observations prompted us to assess the electron diffusion across this particular interfacial assembly by chronoamperometry. Specifically, we applied a potential step from 0 to -0.65 V to the gold substrate and probed the evolution of the current for the reduction of the bipyridinium dications to their radical cations. The fitting of the linear portion of the resulting plot (Figure 5a) to the Cottrell equation^{2c} gives an estimate of $31 \text{ nmol cm}^{-2} \text{ s}^{-1/2}$ for the product of the bipyridinium concentration (c) in the film and the square root of the apparent diffusion coefficient for charge transport (D_A). This value is comparable to the $c\sqrt{D_A}$ reported in the literature for redox polymers incorporating bipyridinium dications.^{11b} In fact, a statistical analysis of 40 independent literature entries^{16–21} shows that the $c\sqrt{D_A}$ of bipyridinium polymers cluster around $30 \text{ nmol cm}^{-2} \text{ s}^{-1/2}$ and rarely extends outside the $1\text{--}60 \text{ nmol cm}^{-2} \text{ s}^{-1/2}$ range.²²

Further inspection of the literature data reveals that the $c\sqrt{D_A}$ values of bipyridinium polymers determined by chronoamperometry are generally 2–5 times smaller than those obtained in steady-state measurements.^{16c,19c,d} As a result, we determined this particular parameter again with an independent technique. Specifically, we maintained the potential of a modified gold electrode at the $E_{1/2}$ (-0.418 V) of the bipyridinium dications for 600 s. After the initial equilibration, we applied an oscillating potential centered at $E_{1/2}$ with an amplitude of 5 mV and probed the impedance of the system, while scanning the frequency from 100 kHz to 0.1 Hz. The resulting impedance profile (Figure 5b) lacks the semicircular region at high frequencies characteristic of a kinetically controlled response. In fact, the negligible charge-transfer resistance implies that the heterogeneous electron transfer to the bipyridinium dications must be relatively fast. By contrast, the semiinfinite and thin-layer regions of the plot are well-defined with linear correlations between the imaginary (Z'') and real (Z') parts of the impedance in both instances. A quantitative analysis²³ of both regions indicates $c\sqrt{D_A}$ to be $71 \text{ nmol cm}^{-2} \text{ s}^{-1/2}$. This value is approximately 2.3 times greater than that determined by chronoamperometry, in agreement with the trends reported in the literature.^{16c,19c,d}

The diffusion of electrons across the bipyridinium dications embedded in our films suggested that we test the ability of these interfacial assemblies to mediate the reduction of electroactive probes in the electrolyte solution. Specifically, we assessed the voltammetric response of $\text{Ru}(\text{NH}_3)_6\text{Cl}_3$ with gold working electrodes preexposed to solutions of **6** over increasing immersion times. This particular ruthenium(III) complex undergoes a reversible reduction with an $E_{1/2}$ of -0.14 V at bare gold (Figure 6a). After the modification of the working electrode with a monolayer of **6**, the reduction wave of the ruthenium centers shifts by -0.14 V (Figure 6b) to overlap the peak for the bipyridinium reduction at -0.37 V (Figure 6c). The reverse scan of the cyclic voltammogram, however, reveals only the back oxidation of the bipyridinium dications at -0.31 V (Figures 6b and 6c). In addition, it shows a broad wave at $+0.03$ V (Figure 3b) instead of the well-defined peak at -0.10 V (Figure 3a) for the ruthenium reoxidation observed at bare gold. At higher bipyridinium surface coverages, obtained by extending the immersion time from 1 to 6 h, the ruthenium centers and bipyridinium dications are again reduced together at -0.42 V (Figures 6d and 6e). The ruthenium back oxidation, however, is now essentially suppressed, and only the bipyridinium back oxidation is observed in the reverse scan. Thus, a bipyridinium film with a Γ that is 4 times greater than the surface coverage of a monolayer can mediate the reduction of the ruthenium centers, while blocking their back oxidation. The rectification imposed on the electron-transfer process by our bipyridinium multilayer is consistent with the ability of similar interfacial assemblies to trap charge.^{19d,24–27} This behavior is a result of (1) the effective coverage of the electrode surface and (2) the mismatch in the reduction potentials of two electroactive units. Indeed, the bipyridinium film coating the electrode prevents the ruthenium(III) complexes from approaching the gold surface. As a result, direct electron transfer from the electrode to the ruthenium(III) centers cannot occur, and their reduction at -0.14 V is not observed (Figure 6d). When the voltage of the gold electrode increases to match the reduction potential of the bipyridinium dications (Figure 7a), electrons diffuse through the interfacial assembly to reach the ruthenium(III) probes at the film/solution interface. Thus, the reduction of the ruthenium(III) centers accompanies that of the bipyridinium dications, and

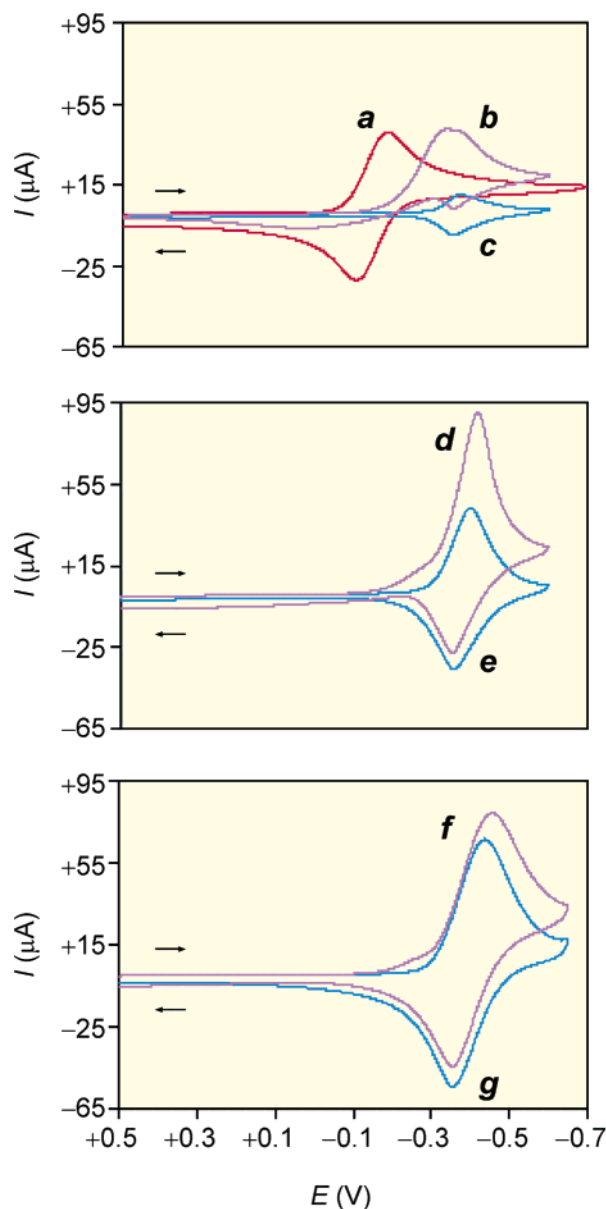


Figure 6. Cyclic voltammograms (0.1 M KCl_{aq}, 100 mV s⁻¹, V vs Ag/AgCl) of Ru(NH₃)₆Cl₃ (5 mM) recorded with gold working electrodes (a) before and after their immersions in solutions of **6** for (b) 1, (d) 6, or (f) 48 h followed by copious rinsing. Cyclic voltammograms (c, e, and g) of the same bipyridinium films in the absence of Ru(NH₃)₆Cl₃ in the electrolyte solution, under otherwise identical conditions.

consistently, the peak current in the corresponding cyclic voltammogram (Figure 6d) is significantly greater than that determined in the absence of Ru(NH₃)₆Cl₃ (Figure 6e). When the voltage of the gold electrode is lowered (Figure 7b), the bipyridinium radical cations reoxidize to the corresponding dication, but the ruthenium(II) centers remain in a reduced state. The mismatch in energy between the bipyridinium lowest unoccupied molecular orbitals (LUMOs) and the filled ruthenium(II) state prevents back electron transfer to the electrode though the bipyridinium dication. It follows that the delivered electrons remain irreversibly trapped in the ruthenium(II) centers.

The ability of the bipyridinium multilayers to mediate the reduction of the ruthenium(III) centers is related to the surface coverage as well as to the scan rate of the voltammogram. When the immersion time of the gold electrode is prolonged from 6 to 48 h, the value of Γ increases by a factor of ca. 3 (Table 1).

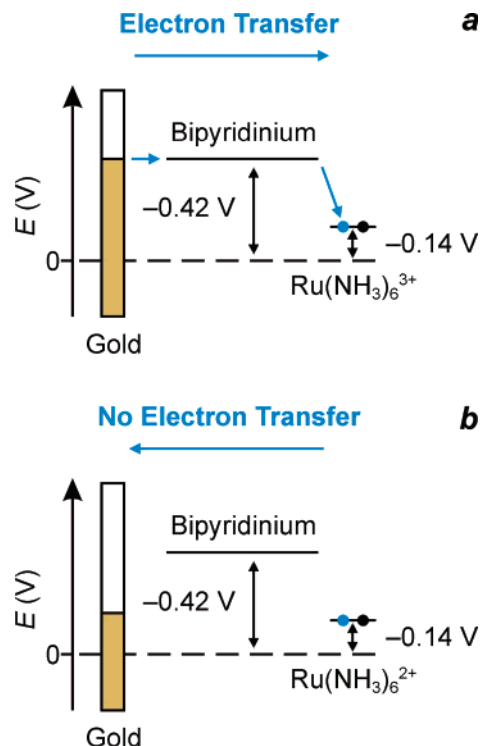


Figure 7. (a) The bipyridinium dication of an electroactive multilayer adsorbed on gold mediate the transfer of electrons from the electrode to a Ru(NH₃)₆³⁺ probe in solution, (b) but prevent electron transfer in the opposite direction. The energy levels (V vs Ag/AgCl) have been estimated from the reduction waves of the cyclic voltammograms a and d in Figure 6.

At this relatively large surface coverage, the reduction of the bipyridinium dication is not exhaustive, when the cyclic voltammogram is recorded at a scan rate of 100 mV s⁻¹. Consistently, the mediation of the ruthenium reduction is not particularly efficient, and the cyclic voltammogram recorded in the presence of Ru(NH₃)₆Cl₃ (Figure 6f) is very similar to the one measured in the absence of the ruthenium(III) probes (Figure 6g). The bipyridinium dication, however, are exhaustively reduced at scan rates smaller than 10 mV s⁻¹ (Figure 4e). Under these conditions, the ruthenium(III) reduction is, indeed, mediated by the bipyridinium film, and the response is similar to the one observed at higher scan rates but lower surface coverage (Figure 6d).

Electroactive Counterions. We isolated the tetracation **6** in the form of a chloride salt and characterized its films on gold in the presence of KCl. Under these conditions, Cl⁻ counterions are presumably incorporated in the interfacial assembly to maintain charge neutrality. Literature reports, however, demonstrate that bipyridinium dication has a strong affinity for Fe(CN)₆⁴⁻ tetraanions.^{25b,e,28–30} On the basis of these observations, we considered the possibility of exchanging the Cl⁻ counterions of our films with electroactive Fe(CN)₆⁴⁻ tetraanions. Comparison of the cyclic voltammograms of a dilute (0.04 mM) solution of K₄Fe(CN)₆ recorded before (Figure 8a) and after (Figure 8b) exposure of a gold working electrode to a solution of **6** confirms the incorporation of the electroactive counterions in the bipyridinium assembly. Indeed, the reversible of oxidation of the Fe(CN)₆^{3/4-} couple can only be observed after modification of the electrode. Presumably, electrostatic interactions between the surface-confined bipyridinium dication and the electroactive tetraanions enrich the local concentration of Fe(CN)₆⁴⁻ at the electrode interface, which is otherwise too dilute for detection. The $E_{1/2}$ for the entrapped anions is +0.19

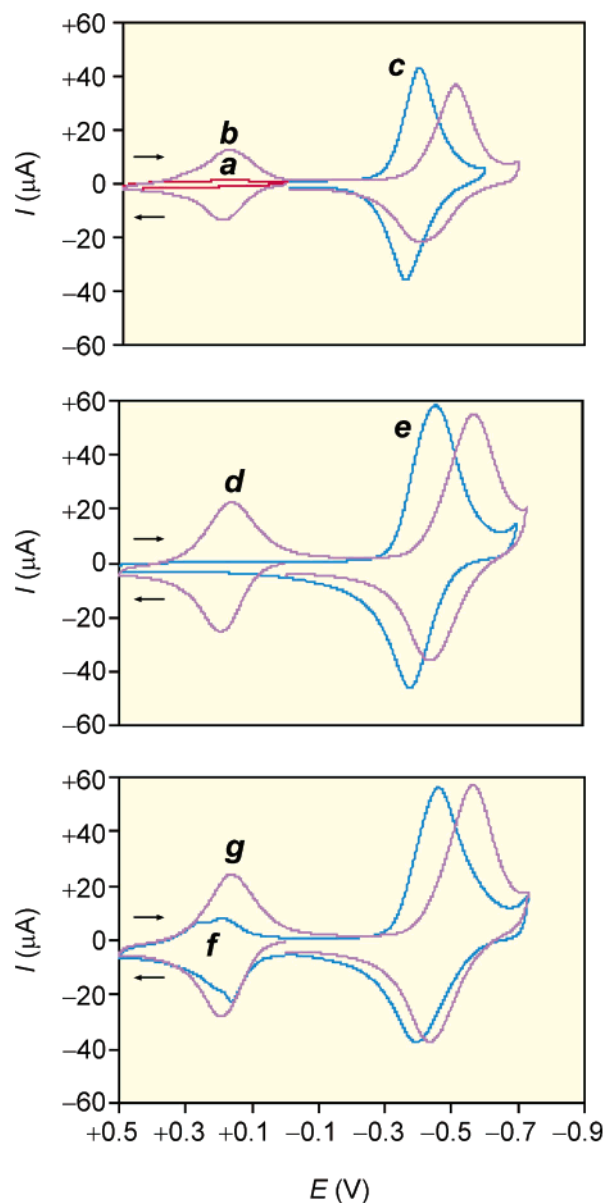


Figure 8. Cyclic voltammograms (0.1 M KCl_{aq}, 100 mV s⁻¹, V vs Ag/AgCl) of K₄Fe(CN)₆ (0.04 mM) recorded with gold working electrodes (a) before and after their immersions in solutions of **6** for (b) 6 or (d) 48 h followed by copious rinsing. Cyclic voltammograms (c and e) of the same bipyridinium films in the absence of K₄Fe(CN)₆ in the electrolyte solution, under otherwise identical conditions. Cyclic voltammograms of K₄Fe(CN)₆ recorded after the immersion of a gold working electrode in a solution of **6** for 48 h, followed by copious rinsing, and the application of a constant potential at (f) -0.73 V for 180 s and then at (g) 0 V for 300 s, under otherwise identical conditions.

V with a ΔE_p of 20 mV. The peak current increases linearly with the scan rate (Figure S8, Supporting Information) with an A of 0.97 in excellent agreement with a thin-layer response. Furthermore, the entrapped anions have a pronounced influence of the bipyridinium response (Figures 8b and 8c). Their $E_{1/2}$ shifts by -0.08 V with an increase in ΔE_p of 66 mV. From the integrals of the Fe(CN)₆⁴⁻ oxidation wave and bipyridinium reduction wave, the ratio between the bipyridinium dication and the Fe(CN)₆⁴⁻ tetraanions can be estimated to be ca. 2:1. This value suggests that most of the Cl⁻ counterions in the bipyridinium films have been replaced by the Fe(CN)₆⁴⁻ tetraanions.

We observed similar results at higher bipyridinium surface coverages, obtained by increasing the immersion time from 6

to 48 h. Again, the cyclic voltammogram (Figure 8d) shows the reversible oxidation of the Fe(CN)₆⁴⁻ tetraanions with an $E_{1/2}$ of +0.19 V and a ΔE_p of 20 mV. The scan-rate dependence of the peak current is close to linearity (Figure S8, Supporting Information) with an A of 0.83. The $E_{1/2}$ of the bipyridinium dication shifts by -0.09 V (Figures 8d and 8e) with an increase in ΔE_p of 54 mV, and the ratio between the electroactive dication and tetraanions is, once more, ca. 2:1. Interestingly, the amount of tetraanions entrapped in the bipyridinium film seems to decrease, if the potential of the gold substrate is maintained at -0.73 V for 180 s. The cyclic voltammogram (Figure 8f), recorded after this treatment, shows a pronounced decrease in the peak current of the Fe(CN)₆⁴⁻ waves. The original peak intensities and shapes, however, are restored, after holding the potential of the gold electrode at 0 V for 300 s (Figure 8g). Presumably, the reduction of the bipyridinium dication to their radical cations weakens the electrostatic interactions holding the Fe(CN)₆⁴⁻ counterions in the film. As a result, a fraction of them is expelled from the interfacial assembly, only to be recaptured after the reoxidation of the bipyridinium dication.

The electroactive Fe(CN)₆⁴⁻ tetraanions trapped in the bipyridinium matrix can in principle transport electrons through the interfacial assembly. To assess their electron transport properties, we determined the $c\sqrt{D_A}$ of films prepared with an immersion time of 48 h by chronoamperometry and impedance measurements. The fitting of the linear portion of the chronoamperometric trace (Figure 9a), recorded after stepping the potential from -0.1 to +0.5 V, to the Cottrell equation^{2c} indicates $c\sqrt{D_A}$ to be 19 nmol cm⁻² s^{-1/2}. The impedance plot (Figure 9b) lacks, once again, the semicircular region at high frequencies typical of a kinetically controlled response. Thus, the heterogeneous electron transfer from the Fe(CN)₆⁴⁻ tetraanions to the electrode is also relatively fast. The semiinfinite and thin-layer regions of the plot are, again, characterized by linear correlations between Z'' and Z' . Their quantitative analysis²³ reveals $c\sqrt{D_A}$ to be 12 nmol cm⁻² s^{-1/2}. This value is close to the one determined by chronoamperometry and approximately twice the literature $c\sqrt{D_A}$ reported for Fe(CN)₆⁴⁻ tetraanions trapped in bipyridinium polymers.²⁹

The bipyridinium multilayers prepared from **6** with an immersion time of 6 h mediate the reduction of Ru(NH₃)₆³⁺ at moderate scan rates (Figure 6d) and can also capture and retain Fe(CN)₆⁴⁻ (Figure 8b). As a result, we explored the influence of the electroactive anions trapped in the bipyridinium assembly on the response of the ruthenium centers in solution. Specifically, we recorded the cyclic voltammogram of an aqueous solution of Ru(NH₃)₆Cl₃ (5 mM) and K₄Fe(CN)₆ (0.04 mM) with a gold working electrode coated by the bipyridinium multilayer. The first segment of the voltammogram (from 0 to +0.5 V) shows the oxidation of the trapped Fe(CN)₆⁴⁻ tetraanions at +0.20 V (Figure 10, peak I). The second segment (from +0.5 to -0.7 V) reveals their back reduction at +0.18 V (Figure 10, peak II) and a wave for the bipyridinium reduction at -0.53 V (Figure 10, peak III). A comparison with the cyclic voltammogram (Figure 8b), recorded in the absence of Ru(NH₃)₆Cl₃ in the electrolyte solution, shows that the $E_{1/2}$ and ΔE_p of the Fe(CN)₆^{3/4-} couple as well as the bipyridinium reduction potential are essentially unchanged. However, the peak current for the bipyridinium wave is significantly higher in the presence Ru(NH₃)₆Cl₃. Thus, the bipyridinium dication is mediating efficiently the reduction of the ruthenium(III) centers in solution. The third segment (from -0.7 to +0.5 V) of the voltammogram shows the back oxidation of the bipyridinium

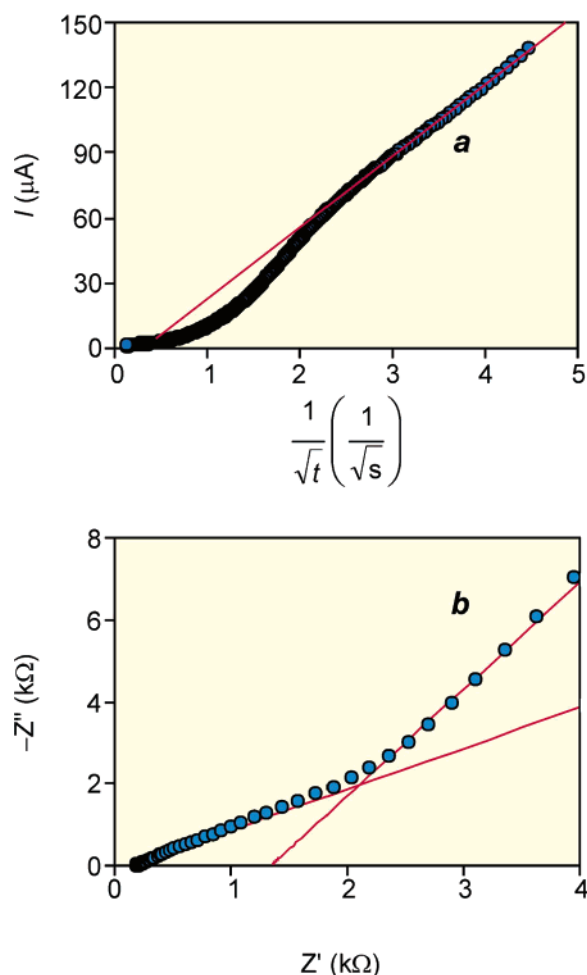


Figure 9. (a) Chronoamperometric ($-0.10 \rightarrow +0.50$ V vs Ag/AgCl) and (b) impedance ($+0.187 \pm 0.005$ V vs Ag/AgCl, 100 kHz–0.1 Hz) plots recorded in KCl_{aq} (0.1 M) containing $\text{K}_4\text{Fe}(\text{CN})_6$ (0.04 mM) after the immersion of gold working electrodes in solutions of **6** for 48 h followed by copious rinsing. The coefficients of determination for the fittings are greater than 0.99.

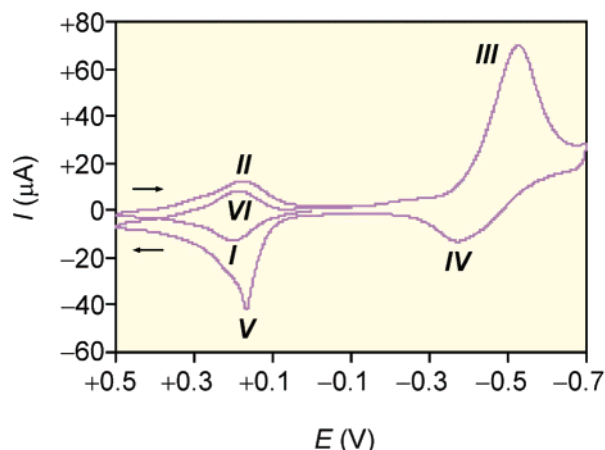


Figure 10. Cyclic voltammograms (0.1 M KCl_{aq} , 100 mV s^{-1} , V vs Ag/AgCl) of $\text{Ru}(\text{NH}_3)_6\text{Cl}_3$ (5 mM) recorded in the presence of $\text{K}_4\text{Fe}(\text{CN})_6$ (0.04 mM) after the immersion of a gold working electrode in a solution of **6** for 48 h followed by copious rinsing.

radical cations at -0.37 V (Figure 10, peak IV) and, again, the oxidation of the $\text{Fe}(\text{CN})_6^{4-}$ tetraanions (Figure 10, peak V). However, the peak current of the $\text{Fe}(\text{CN})_6^{4-}$ oxidation wave in the third scan (Figure 10, peak V) is significantly greater than that in the first (Figure 10, peak I). This observation suggests

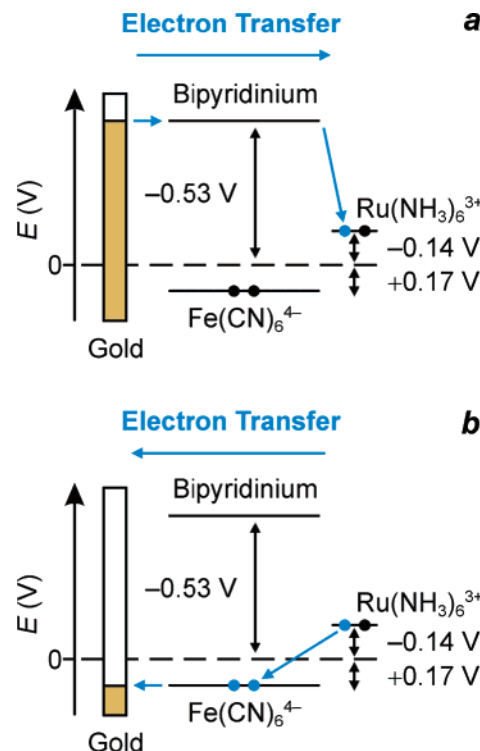


Figure 11. (a) The bipyridinium dications of an electroactive multilayer adsorbed on gold mediate the transfer of electrons from the electrode to a $\text{Ru}(\text{NH}_3)_6^{3+}$ probe in solution. (b) The $\text{Fe}(\text{CN})_6^{4-}$ counterions trapped in the film mediate the electron transfer in the opposite direction. The energy levels (V vs Ag/AgCl) have been estimated from the redox waves of the cyclic voltammogram in Figure 10.

that the $\text{Fe}(\text{CN})_6^{4-}$ tetraanions are mediating the reoxidation of the ruthenium(II) centers, which otherwise remain in a reduced state (Figure 6d). Consistently, the fourth and final segment (from +0.5 to 0 V) shows a much smaller peak current (Figure 10, peak VI) for the back reduction of the $\text{Fe}(\text{CN})_6^{3-}$ trianions.

The influence of the counterions trapped in the interfacial assembly on the response of the ruthenium(III) centers in the electrolyte solution can be explained with the aid of the energy diagrams in Figure 11. The effective coverage of the electrode surface prevents direct electron transfer from the electrode surface to the ruthenium probes. Only when the gold voltage is close to the reduction potential of the bipyridinium dications can electrons be transferred to the ruthenium(III) centers (Figure 11a). Under these conditions, electron hopping through the bipyridinium LUMOs facilitates their diffusion across the film and mediates the reduction of the redox probes in solution. When the gold voltage is lowered, the bipyridinium radical cations are reoxidized, leaving the ruthenium centers in a reduced form. The mismatch in energy between the bipyridinium LUMOs and the ruthenium state prevents back electron transfer, and the delivered electrons remain trapped in the metal complexes. However, they can be released through the $\text{Fe}(\text{CN})_6^{4-}$ tetraanions back to the electrode. Indeed, the oxidation of the $\text{Fe}(\text{CN})_6^{4-}$ tetraanions is accompanied by electron transfer from the ruthenium(II) centers to the resulting $\text{Fe}(\text{CN})_6^{3-}$ trianions (Figure 11b). The overall result is a net flow of electrons from the film/solution interface to the gold electrode. Thus, the bipyridinium assembly can deliver electrons to the ruthenium(III) centers in solution, and the electroactive counterions permit the release of the electrons stored in the solution probes back to the electrode.

Conclusions

Our studies demonstrate that a compound incorporating two bipyridinium dications at its core and two oligomethylene tails with terminal thiol groups adsorbs spontaneously on polycrystalline gold electrodes. The surface coverage of the resulting films increases with the exposure time of the gold substrate to the bipyridinium solution. Films with a monolayer surface coverage and a thin-layer electrochemical response are obtained after only 1 h. The surface coverage grows by 1 order of magnitude, and the response becomes diffusive, when the exposure time is prolonged to 48 h. Control experiments with five model compounds reveal that two bipyridinium dications must be in the molecular skeleton of each building block to lower the solubility in the deposition solvent and encourage multilayer growth. Furthermore, two thiol groups must be appended at the termini of each building block to stabilize the resulting films, presumably, as a result of interlayer disulfide bonding. When both design criteria are satisfied, electroactive multilayers with remarkable stability assemble spontaneously on gold.

Chronoamperometry and impedance measurements demonstrate that the $c\sqrt{D_A}$ values of our self-assembling multilayers are comparable to those of conventional bipyridinium polymers. In both instances, electrons can diffuse from the electrode surface through the bipyridinium dications to the film/solution interface. Consistently, our films mediate efficiently the reduction of $\text{Ru}(\text{NH}_3)_6^{3+}$. However, they prevent the back oxidation of the ruthenium probes, when the bipyridinium surface coverage is sufficiently large. Under these conditions, the assembly of bipyridinium dications imposes rectification on the electron-transfer process. Electrons can migrate from the gold surface to the species in solution but cannot travel in the opposite direction. Nonetheless, the trapped electrons can be released back to the electrode, if the chloride counterions of the interfacial assembly are replaced with $\text{Fe}(\text{CN})_6^{4-}$ tetraanions. Indeed, electrostatic interactions between the bipyridinium dications and the $\text{Fe}(\text{CN})_6^{4-}$ tetraanions encourage the preferential entrapment of these counterions in the polycationic multilayers. In the resulting films, the oxidation of the electroactive tetraanions can be exploited to mediate efficiently the back oxidation of the ruthenium centers. Thus, the ability of our self-assembling multilayers to transport electrons changes with the nature of their anionic partners.

Acknowledgment. We thank the National Science Foundation (CAREER Award CHE-0237578) for financial support and the University of Miami for a Robert E. Maytag Fellowship to J. M.

Supporting Information Available: Experimental procedures for the synthesis of **1–6**, determination of $c\sqrt{D_A}$ from the impedance plots, and scan-rate dependence of the peak current in the cyclic voltammograms of $\text{K}_4\text{Fe}(\text{CN})_6$. This material is available free of charge via the Internet at <http://pubs.acs.org>.

References and Notes

- (1) *Electron Transfer in Chemistry*; Balzani, V., Ed.; Wiley-VCH: Weinheim, 2001.
- (2) (a) *Molecular Design of Electrode Surfaces*; Murray, R. W., Ed.; Wiley: New York, 1992. (b) Bard, A. J. *Integrated Chemical Systems: A Chemical Approach to Nanotechnology*; Wiley: New York, 1994. (c) Bard, A. J.; Faulkner, L. R. *Electrochemical Methods: Fundamentals and Applications*; Wiley: New York, 2001.
- (3) (a) Murray, R. W. *Acc. Chem. Res.* **1980**, *13*, 135–141. (b) Murray, R. W. *Annu. Rev. Mater. Sci.* **1984**, *14*, 145–169. (c) Murray, R. W. *Electroanal. Acta* **1984**, *13*, 191–368. (d) Faulkner, L. R. *Chem. Eng. News* **1984**, 62 (9), 28–45. (e) Chidsey, C. E. D.; Murray, R. W. *Science* **1986**, *231*, 25–31. (f) Wrighton, M. S. *Science* **1986**, *231*, 32–37. (g) Kaneko, M.; Wohrle, D. *Adv. Polym. Sci.* **1988**, *84*, 141–228. (h) Dalton, E. F.; Surridge, N. A.; Jernigan, J. C.; Wilbourn, K. O. *Chem. Phys.* **1990**, *141*, 143–157. (i) Inzelt, G. *Electroanal. Chem.* **1994**, *18*, 89–241. (j) Schumann, W. *Mikrochim. Acta* **1995**, *121*, 1–29. (k) Durst, R. A.; Baumann, A. J.; Murray, R. W.; Buck, R. P.; Andrieux, C. P. *Pure Appl. Chem.* **1997**, *69*, 1317–1323. (l) McQuade, D. T.; Pullen, A. E.; Swager, T. M. *Chem. Rev.* **2000**, *100*, 2537–2574. (m) Klein, L. J.; Peters, D. G. In *Encyclopedia of Analytical Chemistry: Applications, Theory and Instrumentation*; Meyers, R. A., Ed.; Wiley: Chichester, 2000; Vol. 11, pp 10069–10090. (n) Walcarious, A. *Chem. Mater.* **2001**, *13*, 3351–3372.
- (4) (a) Kuhn, H.; Möbius, D. *Angew. Chem., Int. Ed. Engl.* **1971**, *10*, 620–637. (b) Fujihira, M. In *Photochemical Processes in Organized Systems*; Honda, K., Ed.; Elsevier: Amsterdam, 1991; pp 463–482. (c) Fujihira, M. In *Nanostructures Based on Molecular Materials*; Göpel, W.; Ziegler, C., Eds.; VCH: Weinheim, 1992; pp 27–46.
- (5) *Multilayer Thins Films*; Decher, G.; Schlenoff, J. B., Eds.; Wiley-VCH: Weinheim, 2003.
- (6) (a) Ulman, A. *An Introduction to Ultrathin Organic Films*; Academic Press: Boston, 1991. (b) Vos, J. G.; Forster, R. J.; Keyes, T. E. *Interfacial Supramolecular Assemblies*; Wiley: New York, 2003.
- (7) (a) Finklea, H. O. *Electroanal. Chem.* **1996**, *19*, 109–335. (b) Chechik, V.; Stirling, C. J. M. In *The Chemistry of Organic Derivatives of Gold and Silver*; Patai, S.; Rappoport, Z., Eds.; Wiley: Chichester, 1999; pp 551–640. (c) Finklea, H. O. In *Encyclopedia of Analytical Chemistry: Applications, Theory and Instrumentation*; Meyers, R. A., Ed.; Wiley: Chichester, 2000; Vol. 11, pp 10090–10115.
- (8) (a) Kohli, P.; Taylor, K. K.; Harris, J. J.; Blanchard, G. J. *J. Am. Chem. Soc.* **1998**, *120*, 11962–11968. (b) Joo, S. W.; Han, S. W.; Kim, K. *Langmuir* **2000**, *16*, 5391–5396. (c) Joo, S. W.; Han, S. W.; Kim, K. *Mol. Cryst. Liq. Cryst.* **2001**, *371*, 355–358.
- (9) (a) Tour, J. M.; Jones, L., II; Pearson, D. L.; Lamba, J. J. S.; Burgin, T. P.; Whitesides, G. M.; Allara, D. L.; Parikh, A. N.; Atre, S. V. *J. Am. Chem. Soc.* **1995**, *117*, 9529–9534. (b) Weckenmann, U.; Mittler, S.; Naumann, K.; Fischer, R. A. *Langmuir* **2002**, *18*, 5479–5486. (c) Brower, T. L.; Gamo, J. C.; Ulman, A.; Liu, G.-Y.; Yan, C.; Götzhäuser, A.; Grunze, M. *Langmuir* **2002**, *18*, 6207–6216.
- (10) Monk, P. M. S. *The Viologens: Physicochemical Properties, Synthesis and Applications of the Salts of 4,4'-Bipyridine*; Wiley: New York, 1998.
- (11) (a) Raymo, F. M.; Alvarado, R. J.; Pacsial, E. J. *J. Supramol. Chem.* **2002**, *2*, 63–77. (b) Raymo, F. M.; Alvarado, R. J. *Chem. Rec.* **2004**, *3*, 204–218.
- (12) Golan, Y.; Margulis, G.; Rubinstein, I. *Surf. Sci.* **1992**, *264*, 312–326.
- (13) Widrig, C. A.; Majda, M. *Langmuir* **1989**, *5*, 689–695.
- (14) Raymo, F. M.; Alvarado, R. J.; Pacsial, E. J.; Alexander, D. J. *Phys. Chem. B* **2004**, *108*, 8622–8625.
- (15) Pretsch, E.; Clerc, T.; Seibl, J.; Simon, W. *Tables of Spectral Data for Structure Determination of Organic Compounds*; Springer-Verlag: Berlin, 1989.
- (16) (a) Willman, K. W.; Murray, R. W. *J. Electroanal. Chem.* **1982**, *133*, 211–231. (b) Murray, R. W.; Burgmayer, P. J. *Electroanal. Chem.* **1982**, *135*, 335–342. (c) Dalton, E. F.; Murray, R. W. *J. Phys. Chem.* **1991**, *95*, 6383–6389. (d) Terrill, R. H.; Hutchinson, J. E.; Murray, R. W. *J. Phys. Chem. B* **1997**, *101*, 1535–1542.
- (17) (a) Mortimer, R. J.; Anson, F. C. *J. Electroanal. Chem.* **1982**, *138*, 325–341. (b) Martigny, P.; Anson, F. C. *J. Electroanal. Chem.* **1982**, *139*, 383–393.
- (18) (a) Oshaka, T.; Yamamoto, H.; Kaneko, M.; Yamada, A.; Nakamura, M.; Nakamura, S.; Oyama, N. *Bull. Chem. Soc. Jpn.* **1984**, *57*, 1844–1849. (b) Oshaka, T.; Oyama, N.; Sato, K.; Matsuda, H. *J. Electrochem. Soc.* **1985**, *132*, 1873–1879.
- (19) (a) Bookbinder, D. C.; Wrighton, M. S. *J. Electrochem. Soc.* **1983**, *130*, 1080–1087. (b) Dominey, R. N.; Lewis, T.; Wrighton, M. S. *J. Phys. Chem.* **1983**, *87*, 5345–5354. (c) Shu, C.-F.; Wrighton, M. S. In *Electrochemical Surface Science: Molecular Phenomena at Electrode Surfaces*; Soriage, M. P., Ed.; ACS Symposium Series 378; American Chemical Society: Washington, DC, 1988; pp 409–430. (d) Smith, D. K.; Lane, G. A.; Wrighton, M. S. *J. Phys. Chem.* **1988**, *92*, 2616–2628.
- (20) Kopley, L. J.; Bard, A. J. *J. Electrochem. Soc.* **1995**, *142*, 4129–4138.
- (21) Downward, A. J.; Surridge, N. A.; Gould, S.; Meyer, T. J.; Deronzier, A.; Mutet, J.-C. *J. Phys. Chem.* **1990**, *94*, 6754–6764.
- (22) The extraction of D_A from $c\sqrt{D_A}$ requires an independent determination of c . In principle, c can be calculated from Γ and the film thickness (ref 11b). A reliable measurement of the thickness under the same conditions of the electrochemical experiment, however, is a rather challenging task. Furthermore, the thickness might vary during the chronoamperometric

measurement, as the electroactive film changes from a fully oxidized to a fully reduced state. In fact, ellipsometric studies on bipyridinium polysiloxanes revealed the thickness to decrease by ca. 25% upon reduction of the redox-active dications to the corresponding radical cations (ref 20). For these complications, the term $c\sqrt{D_A}$ is often reported in the literature instead of the absolute value of D_A (chapter 8 of ref 2a).

(23) The model employed to extract $c\sqrt{D_A}$ from the impedance plot and the fitted parameters are reported in the Supporting Information.

(24) Denisevich, P.; Willman, K. W.; Murray, R. W. *J. Am. Chem. Soc.* **1981**, *103*, 4727–4737.

(25) (a) Smith, D. K.; Lane, G. A.; Wrighton, M. S. *J. Am. Chem. Soc.* **1986**, *108*, 3522–3525. (b) Smith, D. K.; Tender, L. M.; Lane, G. A.; Licht, S.; Wrighton, M. S. *J. Am. Chem. Soc.* **1989**, *111*, 1099–1105. (c) Hable, C. T.; Crooks, R. M.; Wrighton, M. S. *J. Phys. Chem.* **1989**, *93*, 1190–1192. (d) Wrighton, M. S.; Palmore, G. T. R.; Hable, C. T.; Crooks, R. M.

In *New Aspects of Organic Chemistry I*; Yoshida, Z.; Shiba, T., Ohshiro, Y., Eds.; VCH: Weinheim, 1989; pp 277–302. (e) Hable, C. T.; Crooks, R. M.; Valentine, J. R.; Glasson, R.; Wrighton, M. S. *J. Phys. Chem.* **1993**, *97*, 6060–6065.

(26) Li, Z.; Wang, C. M.; Persaud, L.; Mallouk, T. E. *J. Phys. Chem.* **1988**, *92*, 2592–2597.

(27) Gittins, D. I.; Bethell, D.; Nichols, R. J.; Schiffrin, D. J. *J. Mater. Chem.* **2000**, *10*, 79–83.

(28) (a) Bruce, J. A.; Wrighton, M. S. *J. Am. Chem. Soc.* **1982**, *104*, 74–82. (b) Lewis, N. S.; Wrighton, M. S. *J. Phys. Chem.* **1984**, *88*, 2009–2017.

(29) Mortimer, R. J.; Anson, F. C. *J. Electroanal. Chem.* **1982**, *138*, 325–341.

(30) (a) Miller, C. J.; Majda, M. *Anal. Chem.* **1988**, *60*, 1168–1176. (b) Miller, C. J.; Widrig, C. A.; Charych, D. H.; Majda, M. *J. Phys. Chem.* **1988**, *92*, 1928–1936.